

A Simplified Method for Determination of the Moisture Transfer Coefficient of Concrete

Mehdi Nemati Chari¹ · Mohammad Shekarchizadeh¹

Received: 4 November 2015/Revised: 16 January 2016/Accepted: 10 May 2016/Published online: 21 September 2017
© Iran University of Science and Technology 2017

Abstract The moisture transfer coefficient (MTC) is an important parameter utilized in modeling of moisture ingress into concrete. Test methods for estimating the MTC are generally performed using time-consuming combined experimental–numerical procedures. This paper presents a simple and practical method for the determination of the MTC using only water absorption test results. In this regard, a comprehensive nomograph was constructed based on finite element (FE) analysis of moisture transfer which relates the MTC to the water absorption measurements of concrete specimens. To validate the proposed method, eight concrete mixtures were prepared and their MTCs were obtained using the proposed nomograph and water absorption measurements after 1 and 4 h of immersion. Using the estimated MTCs, a numerical model was applied to predict the water absorption. The subsequent water absorption data resulting from the FE model were compared with the laboratory test results at intervals of 8, 12, 24 and 72 h, with h standing for “hour”. An observed error level up to 5% confirmed the validity of the proposed method.

Keywords Moisture transfer coefficient · Water absorption · Nomograph · Numerical analysis

1 Introduction

Common deterioration problems in concrete structures such as rebar corrosion are mainly associated with the transfer of moisture into concrete during wetting. Modeling of moisture transport in concrete and the subsequent life-cycle analysis of concrete structures also necessitate the prediction of the moisture distribution within unsaturated concrete [1, 2].

Several test methods have been suggested for the determination of the moisture diffusivity and permeability of concrete. Those proposed for estimation of the water absorption rate include measurement of sorptivity [3], water absorption after 30 min [4], penetration depth of water under pressure [5] and water permeability of concrete specimens at a specified pressure [6]. The results obtained from these test methods, however, are not applicable for prediction of the moisture distribution in concrete as well as durability assessment [7–11]. To provide life-cycle analysis and durability assessment, the moisture transfer coefficient, D_w (m^2/s), should be determined; the coefficient is subsequently used as an input parameter in the moisture transport modeling [12–14].

D_w can be calculated from the transient moisture distribution using profile method [14]. Several techniques have been used to measure the moisture distribution profiles. These include slice–dry–weigh [14] and thermal imaging [15] as destructive methods and gamma-ray attenuation [16], neutron radiography [17], nuclear magnetic resonance [18], magnetic resonance imaging [19] and electrical resistivity methods [20] as non-destructive techniques. These non-destructive test methods are usually expensive and difficult to perform. They also require sophisticated facilities which are not available for every contractor [21]. In some cases, the profiles were analyzed

✉ Mohammad Shekarchizadeh
shekarch@ut.ac.ir

¹ School of Civil Engineering, University of Tehran, Tehran, Iran

using a Boltzmann transformation [22, 23] or inverse numerical modeling [24–26] to obtain D_w . In addition, the cup method, according to ASTM E96, is the stationary technique used for the study of water vapor diffusion through a porous material [27, 28]. This technique, however, is time consuming and requires many parallel specimens as the measurements are usually performed at various relative humidity (RH) levels [29, 30].

Due to some disadvantages associated with these techniques such as complexity, high cost, and being time consuming, an alternative technique, namely the gravimetric method, is now a widespread method to follow D_w [31]. In this method, the mass of a small specimen is measured during the exposure to water [32]. An inverse modeling technique is, then, used to evaluate the D_w in porous building materials. The identification of parameters is performed by minimizing the sum of square deviation between the numerical and experimental values of the average moisture content of a specimen at several time intervals [33, 34]. Despite some advantages of this method, a combined experimental–numerical approach is required.

The aim of this study is to develop a practical method for the determination of D_w using a simple experimentation and a nomograph obtained from a numerical analysis. In order to validate the proposed method, an experimental study on the field specimens was conducted. In this regard, the approximated values of D_w of the specimens, obtained from the nomograph, were utilized for the prediction of the water absorption later on using numerical analyses. Then, the predicted water absorption values were compared with the experimental results to validate the accuracy of the proposed method.

2 Moisture Transfer

2.1 Formulation and Background

Several theories have been developed, during the past few decades, for the description of liquid transfer or vapor diffusion through a porous matrix. These were mainly based on the mass, momentum, and energy conservation laws expressed by Darcy's law and Fick's second law of diffusion [35–38]. Depending on the dominant mechanism during water transport, the moisture movement can be expressed in two ways: (a) in the form of the pore evaporable water or (b) in the form of the pore relative humidity [39]. Liquid and vapor flows usually occur in the same direction and are hardly separated in an experiment. However, it is more practical to use one mechanism of moisture transfer, preferably water movement, in the state of water absorption, especially for the modeling of the ion transfer [40]. The major cause of water flow into a porous

material during the water absorption is known to be the capillary forces [41–43]. Capillary action should, therefore, be considered as a liquid form of moisture transport. Although the described water transport is due to the capillary potential gradient and not strictly due to the diffusion process, the diffusion form of the governing differential equation on water transport, for isothermal cases, is as follows [44]:

$$q_m = -D_w \nabla w, \quad (1)$$

where q_m , w and D_w represent the total moisture flow (m/s), the pore water saturation degree, and the equivalent total moisture transfer coefficients (m^2/s) in the form of liquid, respectively.

Neglecting gravitational effects and moisture loss due to hydration, and also considering the mass conservation of water in the concrete pores [45], the rate of moisture transfer per unit area in a certain direction is proportional to the gradient of the moisture concentration in that direction. Consequently, the water saturation degree of concrete or cement paste, w , should satisfy the following partial differential equation [46]:

$$\frac{\partial w}{\partial t} + \nabla \cdot (q_m) - Q_w = 0, \quad (2)$$

where Q_w represents a sink term of evaporable water due to hydration or another chemical reaction. In the present study, assuming no chemical reaction occurs between water and the solid phase of pore structure, a constant solution density, and isothermal conditions, the substitution of Eq. (1) into (2) yields [47, 48]:

$$\frac{\partial w}{\partial t} = D_w \nabla^2 w. \quad (3)$$

The major problem in the accurate determination of D_w is that the moisture movement through cementitious materials considerably depends on the pore moisture content. Some empirical correlations have been proposed to provide an approximation of D_w during moisture gain [49]. Among the proposed correlations, Eq. (4) is more common for modeling the variation of D_w with the value of w of pores in the wetting process [50]:

$$D_w = D_w^d e^{-\beta w}, \quad (4)$$

where D_w^d is the dried-state moisture transfer coefficient during moisture gain (m^2/s) and β is a model parameter that must be determined. According to Eq. (4), D_w decreases during the wetting process of concrete.

2.2 Numerical Modeling of Moisture Transfer

To solve Eq. (3), the residual weight (Galerkin) method was employed using the finite element (FE) technique.

Applying the Galerkin weighted residual method to Eq. (3) yields:

$$[K_w]\{w_j\} + [C_w]\{\dot{w}_j\} = \{f_w\}, \tag{5}$$

where

$$[K_w] = D_w \int_V [B]^T [B] dv + B_w \int_S \{N_j\}^T ds,$$

$$[C_w] = \int_V \{N_j\}^T \{N_j\} dv,$$

$$\{f_w\} = B_w \int_S \{N_j\}^T \{w_{env}\} ds,$$

and N_j , S and V are the shape function, boundary and main domain, respectively. $[B]$ is equal to $\nabla\{N_j\}$, and j is the number of shape function. Equation (5) is integrated over time using a finite difference approximation [51, 52]. B_w is the surface moisture transfer coefficient (m/s) [53], and w_{env} is the value of w at the surface of the concrete. w_{env} is equal to 1 when concrete is exposed to water.

B_w is calculated using the equivalent thickness (l_e) of the concrete adjacent to the real exposed surface from $B_w = D_w/l_e$. Bazant and Najjar [39] suggested, based on the comparison of some analytical data with the experimental results, that the value of the equivalent surface thickness was approximately 0.75 mm. B_w is, therefore, calculated as follows:

$$B_w \text{ (m/s)} = \frac{D_w \text{ (m}^2\text{/s)}}{0.75 \times 10^{-3} \text{ (m)}}. \tag{6}$$

3 Proposed Test Method

3.1 Theoretical Approach

The distribution of water in concrete due to the moisture flux, J_m , at time t_i (Fig. 1a) is presented by the curve shown in Fig. 1b when the moisture ingress into concrete occurs only through the two exposed sides of the specimens in one direction. If the water saturation degree (w) is obtained at several points along the concrete depth using the profile method, the value of D_w can be approximated by fitting Fick's second law of diffusion to the experimental data using Eq. (3).

As an alternative approach, a simple mass measurement was used in the present study to obtain D_w . w^{ave} at time t_i was calculated from the area under the curve of water saturation degree (w). This method is based on the fact that, theoretically, only one definite curve (Fig. 1c) exists [12],

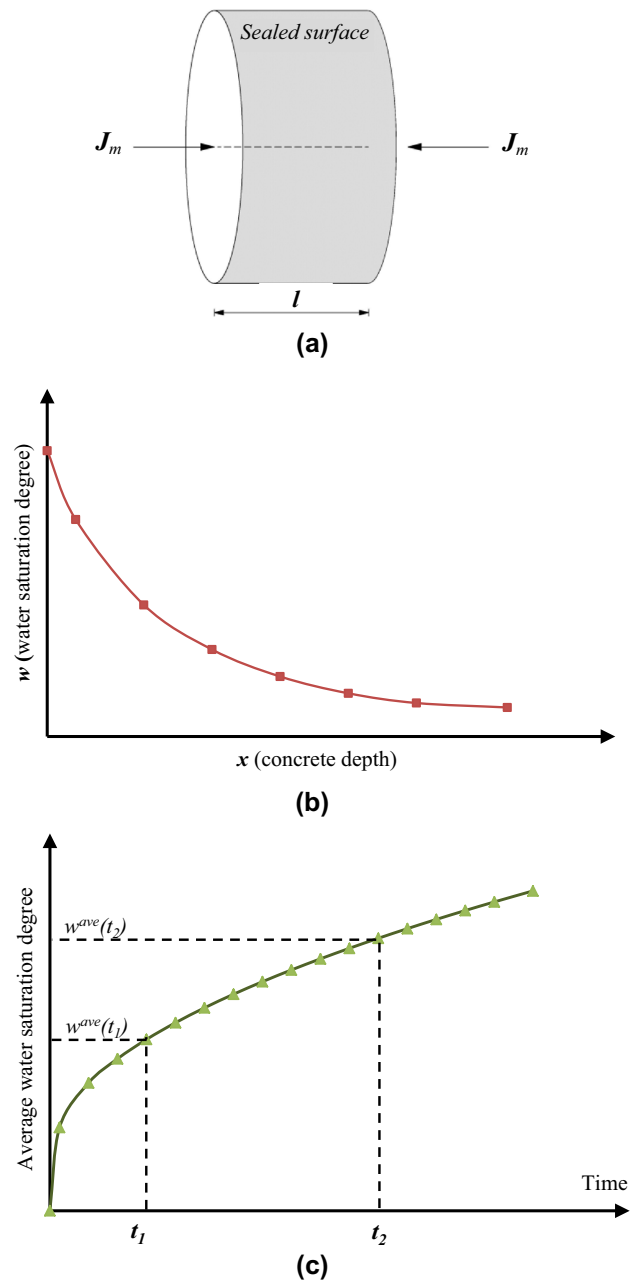


Fig. 1 Typical moisture distribution in concrete: **a** typical 1-D model for moisture transfer into concrete; **b** moisture (w) profile at time t_i ; **c** average water saturation degree (w^{ave}) in the total pores over time

which can be exactly fitted on w^{ave} at t_1 and t_2 using the governing differential equation (Eq. 3) and the moisture transfer coefficient (Eq. 4). In other words, moisture ingress into each specimen of the given D_w^d and β results in the definite values of $w^{ave}(t_1)$ and $w^{ave}(t_2)$ as well as $X = w^{ave}(t_1)$ and $Y = [w^{ave}(t_2)]/[w^{ave}(t_1)]$. Therefore, output sets X – Y can be determined using numerical analysis of one dimensional (1-D) moisture ingress into the concrete test specimen with the specified values of D_w^d , β

and the length of specimen. The relationship between each set X - Y and $D_w^d - \beta$ can be shown by the nomograph. The moisture transfer coefficient can, therefore, be inversely obtained only from the nomograph presented in Fig. 2 using the water absorption of the specimens at t_1 and t_2 and

by assuming 1-D moisture transfer, the moisture dependency of D_w according to Eq. (4) and isothermal conditions.

A pair of times t_1 and t_2 should be selected considering the following remarks:

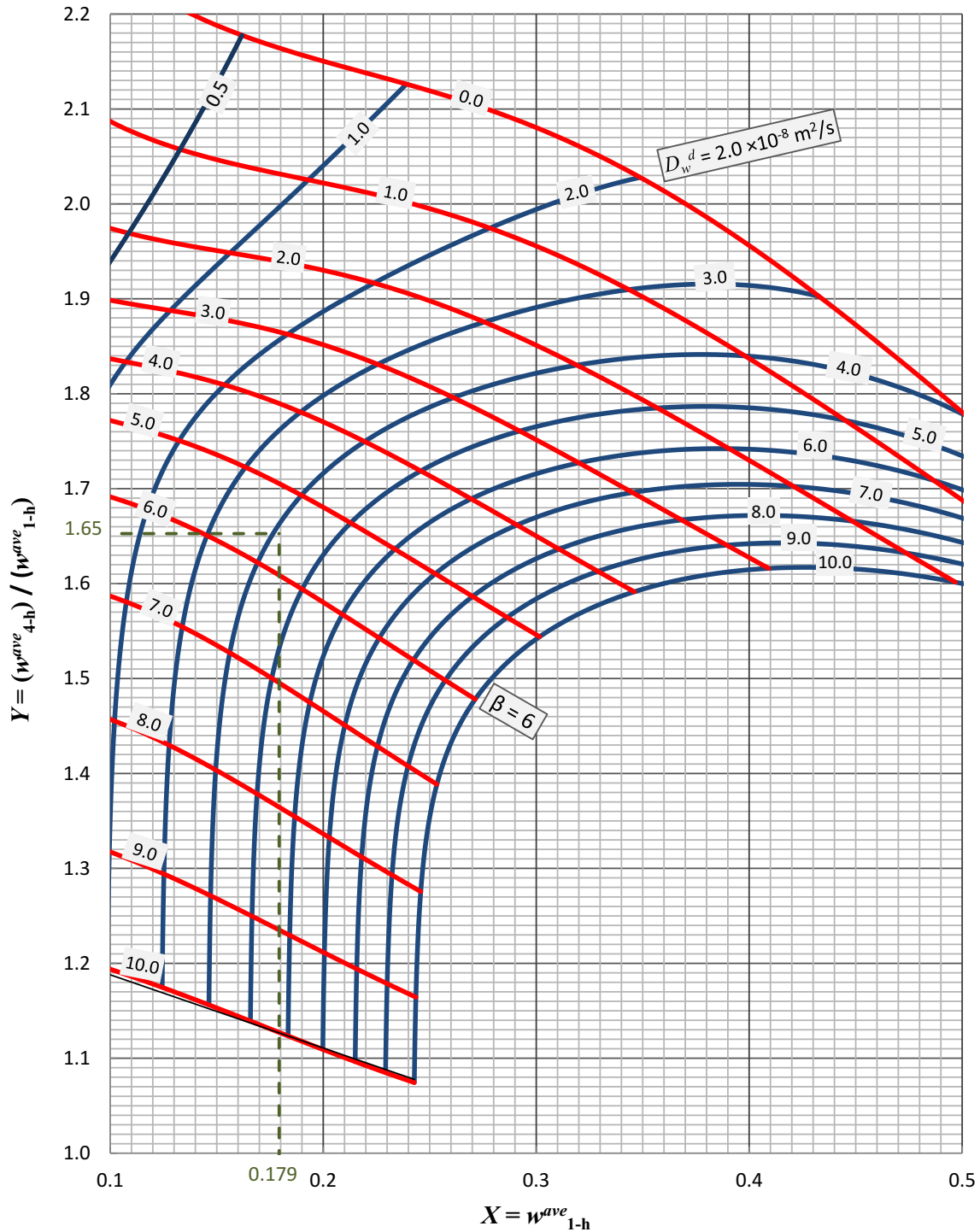


Fig. 2 Nomograph of the water absorption (1-D exposure of a concrete specimen of 50 mm length)

- t_1 should be greater than the minimum extent in order to eliminate the possible effect of boundary condition and exposure surfaces on the test results.
- t_2 becomes in the range of common daily work time, wherein $w^{ave}(t_2)$ is meaningfully greater in comparison with $w^{ave}(t_1)$.

In this paper, 1 and 4 h were selected as t_1 and t_2 , respectively.

3.2 Developing the Nomograph of Water Absorption

To develop the data required for the nomograph of the water absorption, a finite element-based numerical study was conducted. The FE model solved the governing equation of the moisture transport during the wetting. Because the wetting process affects two faces of the concrete specimens, it was necessary to consider the moisture flux to exposed faces of the specimen as the boundary condition. Moreover, the concrete material was assumed to be isotropic. The effect of hydration was neglected during the tests.

A numerical analysis was performed using a 1-D FE model. The input parameters of the model are presented in Table 1. As schematically shown in Fig. 1a, a concrete cylindrical specimen with a length of 50 mm was modeled as a reference. In Eqs. (7 and 8), X and Y of the specimen were computed using different parameters of D_w and then presented in the form of a nomograph (Fig. 2). Parameters D_w^d and β were varied from 5×10^{-9} to 1×10^{-7} m²/s and from zero to 10, respectively, in order to obtain a nomograph covering a wide range of moisture transfer coefficient parameters:

Table 1 Inputs and outputs of the numerical model

Parameters	Value
Input variables	
D_w^d ^a	0.5, 1, 2, 3, 4, 5, 6, 7, 8, 9, 10 $\times 10^{-8}$ m ² /s
β ^b	0, 1, 2, 3, 4, 5, 6, 7, 8, 9, 10
B_w	D_w (m ² /s) in exposed surface/0.75 (mm)
$w(t = 0)$	0.0
w_{env}	1.0
Model output	
$w(x = x_i, t = t_i)$	TBD
$w^{ave}(t = t_i)$	TBD

TBD to be determined

^a β was varied between 0 and 10 in steps of 0.1 for each specified D_w^d

^b D_w^d was varied between 0.5 and 10×10^{-8} m²/s in steps of 0.1 for each specified β

$$X = w_{1-h}^{ave} = \frac{A_1}{A_t}, \tag{7}$$

$$Y = \frac{w_{4-h}^{ave}}{w_{1-h}^{ave}} = \frac{A_2}{A_1}, \tag{8}$$

where A_1 , A_2 and A_t are the 1 h, 4 h and total water absorption (%) values, respectively.

Each blue graph (with constant D_w^d) was drawn using X and Y resulting from a series of analyses, wherein D_w^d was constant and β varied from zero to 10. Similarly, each red graph (with constant β) was drawn using X and Y resulting from a series of analyses, wherein β was constant and D_w^d varied from 5×10^{-9} to 1×10^{-7} m²/s.

These graphs demonstrate a nonlinear interaction of input and output variables on the water absorption. It is suggested, based on the nomograph of Fig. 2, that in general, variations of D_w^d and β are directly related to those of X and Y . Therefore, an increase in β (at a constant value of D_w^d) results in a decrease of the values of both X and Y . In addition, an increase in D_w^d (at a constant value of β) causes an increase in X and a drop in Y . In the range of analyses performed in this study, Y is lower than 1.5 when β is greater than 8. The increase in Y -value would be negligible for high values of β . It is due to the considerable decrease of D_w by increasing β values.

For the approximation of the values of D_w^d and β , the values of X and Y were first calculated using the 1 h, 4 h and total water absorption values. A vertical line perpendicular to the X axis and a horizontal line perpendicular to the Y axis were then drawn on the nomograph, and their intersection point (P) was determined. Two curves parallel to the blue and red curves were drawn so that their intersection occurs at point P . The values of D_w^d and β are then determined by an interpolation.

Variation of the length of specimen likely affects the amount of absorbed water at t_1 and t_2 . A correction of the water absorption values of specimens with the length of l_i (mm) is, therefore, required to obtain the water absorption values of an equivalent 50-mm-long (l_{50}) specimen. The specimens with lengths of 25, 40, 45, 47.5, 52.5, 55, 60 and 75 mm were analyzed in addition to the reference specimen (with a length of 50 mm). The average length correction factors (LCF) of w^{ave} were calculated (Table 2), and the correlated equations were established (Eq. 9). The high correlation ($R^2 > 0.99$) for these relationships indicated a linear dependency of LCF to l_i/l_{50} in the range of the present analyses.

$$LCF = \begin{cases} 0.953 \left(\frac{l_i}{l_{50}}\right) + 0.050 & \text{for } w_{1-h} \\ 0.795 \left(\frac{l_i}{l_{50}}\right) + 0.210 & \text{for } w_{4-h} \end{cases} \tag{9}$$

Table 2 Specimen length correction factors for the average degree of saturation

Specimen length, l_i (mm)	l_i/l_{50}	Length correction factor (average ^a), LCF		Length correction factor (standard deviation ^b), LCF _{SD}	
		w_{1-h}^{ave}	w_{4-h}^{ave}	w_{1-h}^{ave}	w_{4-h}^{ave}
25.0	0.5	0.537	0.617	0.047	0.047
40.0	0.8	0.809	0.845	0.012	0.042
45.0	0.9	0.904	0.921	0.005	0.021
47.5	0.95	0.952	0.960	0.002	0.010
50.0 ^c	1	1.000	1.000	–	–
52.5	1.05	1.048	1.041	0.002	0.010
55.0	1.1	1.097	1.089	0.004	0.012
60.0	1.2	1.194	1.165	0.007	0.037
75.0	1.5	1.487	1.409	0.016	0.043

^aAverage correction factors calculated based on more than 200 numerical analyses

^bStandard deviation of the correction factors for more than 200 numerical analyses

^cReference length of the concrete specimen

The lower standard deviation of LCF (LCF_{SD}) obtained from more than 200 analyses indicates that LCFs of specimens with different D_w^d and β were not considerable. Therefore, the value of w^{ave} ($t = 1$ and 4 h) of a specimen of a length between 25 and 75 mm can be transformed to w^{ave} ($t = 1$ and 4 h) of a 50-mm-long specimen. For example, if the 1 h, 4 h and total water absorptions of a 50-mm-long specimen are 0.98, 1.62 and 4.97%, respectively, then D_w^d and β can be approximated from the nomograph shown in Fig. 2. In this example, X and Y are 0.179 and 1.65, respectively. Considering an X -value of 0.179 on the horizontal axis and a Y -value of 1.65 on the vertical axis of Fig. 2, D_w^d and β could be estimated as 4.1×10^{-8} m²/s and 5.6, respectively.

3.3 Sensitivity Analysis

The variation of specimen sizes and balance accuracies is likely to result in some errors in X and Y and consequently in the estimation of D_w^d and β . A sensitivity analysis was performed to estimate the effect of variations in X and Y on the values of D_w^d and β . The study was based on the calculation of the elasticity of the required parameters. The elasticity provides an estimation of the relative importance (η) of the variations of parameters on the method output. The elasticity is calculated as [12]:

$$\eta = \frac{\Delta Y}{\Delta P} \cdot \frac{\bar{P}}{\bar{Y}}, \quad (10)$$

where \bar{Y} is the output of the proposed method estimated by parameter \bar{P} . ΔY is the variation in the output of the method due to the input parameter variation (ΔP).

Data provided in the previous example (see Sect. 3.3) were utilized for the sensitivity analysis. The input parameters were considered as X and Y , each with a variation of $\pm 5\%$. The ratio of $\bar{P}/\Delta P = 10.0$ was also assumed. The parameters of the moisture transfer coefficient, including D_w^d and β , were considered as the output parameters. The results of the sensitivity analysis are presented in Table 3. It is suggested, based on the results, that the model is significantly sensitive to the Y values. It was, however, less sensitive to the variations of X values. A 5% variation in Y values resulted in 16 and 15% differences in D_w^d and β , respectively. A similar variation in the X values, however, resulted in 7 and 1% differences in D_w^d and β , respectively. The significant dependence on the Y values indicates that special attention must be directed to the estimation of this parameter during the water absorption measurements.

4 Validation Procedure of the Method

4.1 Experimentation

An experimental study was conducted on concrete specimens hydrated for 4 years in order to demonstrate the feasibility of the proposed method. Concrete specimens with various mixture proportions were considered. These include plain concrete mixtures and those containing silica fume and natural zeolite. The mixture constituents of all proportions as well as the fresh and hardened properties of the concrete mixes are presented in Tables 4 and 5, respectively. The chemical analysis of cementitious materials is also provided in Table 6. Fine and coarse

Table 3 Results of the sensitivity analysis

Parameter	Input parameters			Method outputs									
				D_w^d					β				
	\bar{P}	$\bar{P} - 5\%$	$\bar{P} + 5\%$	\bar{Y}	ΔY	$\Delta Y/\bar{Y}$	η	$5\% \times \eta$	\bar{Y}	ΔY	$\Delta Y/\bar{Y}$	η	$5\% \times \eta$
X	0.179	0.170	0.188	4.1	0.6	0.146	1.46	7	5.6	0.1	0.018	0.18	1
Y	1.65	1.57	1.73	4.1	1.3	0.317	3.17	16	5.6	1.7	0.304	3.04	15

Table 4 Concrete mixture proportions

Code	T1-45	T2-40	T2-45	T2-50	T2-55	T5-45	SF7.5	Z10
Cement (kg/m ³)	350	350	350	350	350	350	324	315
Cement type	I	II	II	II	II	V	II	II
Silica fume (kg/m ³)	–	–	–	–	–	–	26	–
Zeolite (kg/m ³)	–	–	–	–	–	–	–	35
Water (kg/m ³)	158	140	158	175	193	158	158	158
w/cm	0.45	0.40	0.45	0.50	0.55	0.45	0.45	0.45
Fine aggregate ^a (kg/m ³)	936	956	936	913	890	936	936	936
Coarse aggregate ^a ($D_{max} = 19$ mm) (kg/m ³)	864	884	864	842	821	864	864	864
Super-plasticizer (kg/m ³)	0.70	0.70	0.28	–	–	0.35	1.19	1.05

^aAggregates were saturated surface dry

Table 5 Fresh and hardened concrete test results

Code	T1-45	T2-40	T2-45	T2-50	T2-55	T5-45	SF7.5	Z10
Slump (cm)	9.5	11.0	12.0	16.0	22.0	9.0	12.0	10.5
Air content (%)	2.2	3.0	3.2	3.2	3.3	1.9	2.2	3.4
Compressive strength (MPa)								
7 days	33.1	30.4	28.0	22.4	17.3	23.1	31.0	25.9
28 days	40.0	42.7	39.1	34.1	31.1	24.9	47.4	39.2
90 days	46.9	49.0	44.6	40.3	35.2	31.8	52.1	44.7
1 year	53.1	51.0	48.9	45.4	41.3	43.2	58.6	52.2
4 years	54.8	53.1	51.7	47.7	42.6	45.3	62.3	56.3

aggregates were prepared from siliceous–calcareous riverbed aggregate with values of the saturated surface dried (SSD) specific gravity and the water absorption of 2.55 and 2.8%, respectively, for the fine aggregate, and 2.57 and 1.6%, respectively, for the coarse aggregate.

A total of 24 concrete cores with a diameter of 69 mm and a length between 45 and 55 mm were drilled and then trimmed for measuring the water absorption at specified times. The side areas of the specimens were sealed with epoxy coat to simulate the 1-D moisture transport conditions.

All specimens were first saturated and then oven-dried to a constant mass at a temperature of 110 ± 5 °C, followed by cooling in a desiccator to a temperature of

23 ± 2 °C. The drying conditions of the specimens were assured by comparing the weight of the dried specimens at a temperature of 110 ± 5 °C with the weight of the cooled specimens at a temperature of 23 ± 2 °C. The difference between the weight of the oven-dried specimen and that of the cooled specimen was very small in all cases. The specimens were then immersed in water at a temperature of 23 ± 2 °C, and the weights of the specimens were measured after 1 and 4 h. The average pore water saturation degree (w^{ave}) was calculated from the amount of water available in the concrete divided by the total water required to saturate the dried specimen. The water absorption test results of the specimens are presented in Table 7.

Table 6 Chemical composition of cementitious materials

Composition (wt.%)	Cement type I	Cement type II	Cement type V	Silica fume	Natural zeolite
CaO	65.7	63.8	60.5	3.1	3.8
SiO ₂	20.3	24.4	20.5	86.2	63.1
Al ₂ O ₃	5.7	3.8	3.6	1.4	11.0
Fe ₂ O ₃	3.3	3.1	4.2	0.2	0.4
SO ₃	1.8	1.5	2.0	0.3	0.1
MgO	1.6	4.4	5.4	1.3	1.6
K ₂ O	0.75	0.79	0.69	–	–
Na ₂ O	0.12	0.08	0.01	–	–
LOI	1.1	1.1	3.0	1.2	8.5
IR	0.45	0.32	0.74		
C ₃ S	65	55	55	–	–
C ₂ S	9	23	18	–	–
C ₃ A	9	5	2	–	–
C ₄ AF	5	9	13	–	–

LOI loss on ignition, *IR* insoluble residue

Table 7 Water absorption test results

Specimen no.	Mixture code	Saturated weight (g)	Dried weight (g)	Total water absorption (%)	Specimen length (mm)	w^{ave} ($t_1 = 1$ h)	w^{ave} ($t_2 = 4$ h)
1	T1-45	475.6	447.0	6.40	54.6	0.196	0.346
2	T1-45	467.9	437.0	7.07	54.0	0.219	0.424
3	T1-45	479.6	446.5	7.41	55.9	0.214	0.411
4	T2-40	409.3	389.4	5.11	47.5	0.128	0.244
5	T2-40	409.2	391.0	4.65	48.7	0.127	0.238
6	T2-40	423.0	405.9	4.21	50.2	0.129	0.245
7	T2-45	410.6	385.5	6.51	48.0	0.152	0.279
8	T2-45	436.5	411.2	6.15	50.4	0.167	0.306
9	T2-45	441.4	417.1	5.83	51.8	0.179	0.309
10	T2-50	434.0	408.4	6.27	50.1	0.195	0.395
11	T2-50	443.3	417.4	6.21	51.6	0.219	0.440
12	T2-50	443.5	416.4	6.51	51.8	0.224	0.432
13	T2-55	414.2	387.9	6.78	48.3	0.306	0.570
14	T2-55	481.7	452.1	6.55	55.4	0.298	0.544
15	T2-55	463.0	433.9	6.71	53.5	0.332	0.625
16	T5-45	472.6	444.6	6.30	54.4	0.206	0.379
17	T5-45	460.7	434.0	6.15	53.4	0.257	0.453
18	T5-45	439.3	411.5	6.76	51.7	0.260	0.482
19	SF7.5	455.1	435.8	4.43	54.6	0.127	0.233
20	SF7.5	470.1	454.5	3.43	55.0	0.164	0.288
21	SF7.5	462.7	441.6	4.78	55.1	0.126	0.234
22	Z10	444.4	431.9	2.89	52.9	0.162	0.280
23	Z10	441.5	432.3	2.13	53.7	0.168	0.278
24	Z10	443.1	434.4	2.00	53.0	0.158	0.276

4.2 Estimation of the Moisture Transfer Coefficient Using the Nomograph

The LCFs of the specimens were calculated using the correlated equation presented in Eq. (9). D_w^d and β were then approximated using the nomograph (Fig. 2) and the corrected w^{ave} at $t_1 = 1$ h and $t_2 = 4$ h (Table 8). In this study, the values of D_w^d and β related to the tested specimens varied from 0.8×10^{-8} to 4.7×10^{-8} m²/s and from 1.0 to 5.5, respectively. The average values of D_w^d and β for Portland cement concrete mixtures were approximately 2.4×10^{-8} m²/s and 2.5, respectively. However, the average values of D_w^d and β obtained for the specimens containing silica fume or natural zeolite were 2.7×10^{-8} m²/s and 4.5, respectively. This difference is likely due to the smaller pore diameter as well as lower porosity of the interfacial transition zone in the mixtures containing silica fume or natural zeolite.

The average saturated state D_w of the specimens containing silica fume or natural zeolite was significantly lower than the ones without pozzolanic materials. This result is consistent with those suggested by Morgan [54] and Roy et al. [55]. These researchers reported that silica fume concrete had a lower rate of water absorption compared to the mixtures without silica fume.

4.3 Validation of the Proposed Method

The approximated parameters of the moisture transfer coefficient were applied to predict w^{ave} of each specimen later using an FE numerical analysis. The water absorption values were measured after 8, 12, 24 and 72 h. The comparison of the experimentally measured values of w^{ave} after $t_2 = 4$ h with the numerical predictions is presented in Table 9. The differences between the model predictions and experimental test results of all tested specimens were

Table 8 Approximated moisture diffusion coefficients

Specimen no.	Correction factors (LCF)		Corrected degree of saturation		D_w^d ($\times 10^{-8}$ m ² /s)	β	D_w ($\times 10^{-10}$ m ² /s) (saturated state)
	w_{1-h}^{ave}	w_{4-h}^{ave}	w_{1-h}^{ave}	w_{4-h}^{ave}			
1	1.090	1.078	0.214	0.373	3.6	3.9	7.3
2	1.080	1.069	0.236	0.453	2.0	1.7	36.5
3	1.116	1.099	0.239	0.452	2.1	1.9	31.4
4	0.956	0.966	0.122	0.236	0.8	2.8	4.9
5	0.979	0.985	0.124	0.234	1.0	3.2	4.1
6	1.006	1.007	0.130	0.247	1.0	2.9	5.5
7	0.966	0.974	0.147	0.272	1.6	3.7	4.0
8	1.010	1.011	0.169	0.309	1.7	3.0	8.5
9	1.038	1.034	0.186	0.319	3.6	4.7	3.3
10	1.005	1.007	0.196	0.397	1.0	1.0	36.8
11	1.033	1.030	0.226	0.453	1.4	1.0	51.5
12	1.036	1.033	0.232	0.446	2.0	1.8	33.1
13	0.970	0.977	0.297	0.557	3.3	1.9	49.4
14	1.107	1.091	0.330	0.594	4.1	1.9	61.3
15	1.070	1.061	0.355	0.664	3.3	1.1	109.8
16	1.087	1.075	0.224	0.407	2.9	3.0	14.4
17	1.067	1.059	0.274	0.480	4.7	3.2	19.2
18	1.035	1.032	0.269	0.497	3.2	2.3	32.1
Average—Portland cement					2.4	2.5	28.5
19	1.090	1.077	0.138	0.251	1.5	3.8	3.4
20	1.099	1.085	0.180	0.313	3.0	4.4	3.7
21	1.100	1.086	0.139	0.254	1.4	3.5	4.2
22	1.058	1.051	0.171	0.294	3.1	4.8	2.6
23	1.074	1.064	0.180	0.296	4.0	5.5	1.6
24	1.060	1.052	0.167	0.290	2.9	4.7	2.6
Average—Portland cement and silica fume or natural zeolite					2.7	4.5	3.0

Table 9 Comparison of the experimental results with the numerical prediction

Specimen no.	Average degree of saturation (w^{ave})								Error (%)			
	Experimental results				Numerical prediction							
	8 h	12 h	24 h	72 h	8 h	12 h	24 h	72 h	8 h	12 h	24 h	72 h
1	0.343	0.404	0.533	0.792	0.332	0.402	0.540	0.771	3	1	1	3
2	0.322	0.398	0.517	0.771	0.331	0.398	0.531	0.753	3	0	3	2
3	0.349	0.409	0.534	0.798	0.344	0.414	0.553	0.780	2	1	4	2
4	0.372	0.435	0.560	0.838	0.376	0.446	0.576	0.799	1	2	3	5
5	0.406	0.468	0.596	0.860	0.414	0.489	0.624	0.825	2	4	5	4
6	0.402	0.463	0.583	0.811	0.412	0.477	0.593	0.774	2	3	2	5
7	0.538	0.635	0.808	0.969	0.546	0.652	0.829	0.982	2	3	3	1
8	0.598	0.701	0.865	0.970	0.619	0.726	0.888	0.993	4	4	3	2
9	0.580	0.680	0.857	0.976	0.591	0.688	0.843	0.979	2	1	2	0
10	0.731	0.824	0.930	0.983	0.730	0.817	0.934	0.997	0	1	0	1
11	0.701	0.790	0.914	0.981	0.730	0.817	0.934	0.997	4	3	2	2
12	0.808	0.898	0.949	0.982	0.806	0.890	0.977	1.000	0	1	3	2
13	0.453	0.525	0.655	0.896	0.458	0.531	0.660	0.855	1	1	1	5
14	0.557	0.654	0.814	0.975	0.584	0.682	0.840	0.979	5	4	3	0
15	0.545	0.636	0.804	0.976	0.552	0.648	0.807	0.966	1	2	0	1
16	0.499	0.578	0.732	0.946	0.505	0.588	0.730	0.912	1	2	0	4
17	0.573	0.652	0.792	0.954	0.590	0.672	0.803	0.950	3	3	1	0
18	0.625	0.711	0.857	0.973	0.634	0.724	0.862	0.981	1	2	1	1
Average									2			
19	0.314	0.371	0.498	0.752	0.318	0.381	0.504	0.712	1	3	1	5
20	0.373	0.428	0.542	0.787	0.384	0.443	0.561	0.759	3	4	4	4
21	0.316	0.372	0.498	0.767	0.324	0.390	0.517	0.732	3	5	4	5
22	0.365	0.420	0.528	0.766	0.374	0.437	0.551	0.734	3	4	4	4
23	0.370	0.418	0.535	0.731	0.365	0.422	0.527	0.697	1	1	2	5
24	0.356	0.418	0.527	0.765	0.370	0.433	0.548	0.733	4	4	4	4
Average									3			

equal or lower than 5%. This result demonstrates that the approximated D_w^d and β had an acceptable precision and that the proposed method is able to accurately estimate the values of D_w^d and β and consequently D_w . The slight differences observed in the calculated errors may be related to the lower water absorption of the mixtures containing silica fume or natural zeolite as well as the inherent error in the experimental measurements.

5 Discussion

The proposed method for the estimation of MTC is associated with some errors. Comparison of the test results to the ones obtained from FEM model showed that the average error is lower than 3%. However, other methods based on the combined experimental–numerical procedures like the traditional method encountered similar errors as well. The method applied by Samson et al. [12] resulted in errors up to 5% and more in some measurements.

Minimizing the sum of square of differences between the numerical and measured data was where the error arises. Since the ability for employing the specimens with different dimensions was a strong point of the method utilized by Samson et al. [12], a relationship was presented in the proposed method to correct the measurements of cylindrical specimens of different thickness values.

Comparison of the proposed method with traditional combined experimental–numerical method like the one in Ref. [12] showed an acceptable level of accuracy and flexibility. Moreover, the estimation needed in the proposed method is more rapid and economical in comparison with the traditional methods.

6 Conclusion

In the present paper, a practical method was proposed to estimate the moisture transfer coefficient of concrete (D_w) using water absorption measurements of concrete

specimens after 1 and 4 h of immersion in water as well as the proposed nomograph. The sensitivity analysis of the proposed method indicated that the estimated D_w was significantly sensitive to the ratio of the water absorption obtained after 4 h to those obtained after 1 h. It was, however, less sensitive to the variation of 1 h water absorption measurements as an input parameter. A comparison between the water absorption measurements after 4 h of immersion with those obtained from the numerical simulation using the estimated D_w validated the method accuracy.

Acknowledgements This work was supported by the Construction Materials Institute (CMI), Faculty of Civil Engineering, University of Tehran. The authors are grateful to Dr. Jafar Sobhani and Eng. Majid Nemati Chari for their contribution to the test program of this study.

References

- Wang L, Ueda T (2011) Mesoscale modeling of water penetration into concrete by capillary absorption. *Ocean Eng* 38(4):519–528
- Kameche ZA, Ghomari F, Choinska M, Khelidj A (2014) Assessment of liquid water and gas permeabilities of partially saturated ordinary concrete. *Constr Build Mater* 65(29):551–565
- ASTM C1585-13 (2013) Standard test method for measurement of rate of absorption of water by hydraulic-cement concretes, American society for testing and materials, Philadelphia, USA
- BS 1881, Part 122 (2011) Testing concrete: method for determination of water absorption. London, BSI
- BS EN 12390-8 (2009) Testing hardened concrete: Depth of penetration of water under pressure, London, BSI
- CRD-C 48 (1992) Standard test method for water permeability of concrete. US Army Corps of Engineers
- Tasdemir C (2003) Combined effects of mineral admixtures and curing conditions on the sorptivity coefficient of concrete. *Cem Concr Res* 33(10):1637–1642
- Neithalath N (2006) Analysis of moisture transport in mortars and concrete using sorption-diffusion approach. *ACI Mater J* 103(3):209–217
- Lanzón M, García-Ruiz PA (2009) Evaluation of capillary water absorption in rendering mortars made with powdered water-proofing additives. *Constr Build Mater* 23(10):3287–3291
- Castro J, Bentz D, Weiss J (2011) Effect of sample conditioning on the water absorption of concrete. *Cement Concr Compos* 33(8):805–813
- Basheer L, Cleland DJ (2011) Durability and water absorption properties of surface treated concretes. *Mater Struct* 44(5):957–967
- Samson E, Maleki K, Marchand J, Zhang T (2008) Determination of the water diffusivity of concrete using drying/absorption test results. *J Test Eval* 5(7):1–12
- Oh BH, Cha SW (2004) Nonlinear analysis of temperature and moisture distributions in early-age concrete structures based on degree of hydration. *ACI Mater J* 100(5):361–370
- Janz M (1997) Methods of measuring the moisture diffusivity at high moisture levels. University of Lund, Lund Institute of technology, Division of Building Materials, Report TVBM-3076
- Sosoro M, Reinhardt HW (1995) Thermal imaging of hazardous organic fluids in concrete. *Mater Struct* 28(9):526–533
- Nizovtsev MI, Stankus SV, Sterlyagov AN, Terekhov VI, Khairulin RA (2005) Experimental determination of the diffusivities of moisture in porous materials in capillary and sorption moistening. *J Eng Phys Thermophys* 78(1):68–74
- Hanzic L, Kosec L, Anzel I (2010) Capillary absorption in concrete and the Lucas-Washburn equation. *Cement Concr Compos* 32(1):84–91
- Pel L, Hazrati K, Kopinga K, Marchand J (1998) Water absorption in mortar determined by NMR. *Magn Reson Imaging* 16(5–6):525–528
- Wolter B, Krus M (2005) Moisture measuring with nuclear magnetic resonance (NMR), electromagnetic aquametry. Springer, Berlin, pp 491–515
- Shekarchi M, Debicki G, Billard Y, Coudert L (2003) Heat and mass transfer of high performance concrete for reactor containment under sever accident condition. *Fire Technol* 39(1):63–71
- Janz M (2002) Moisture diffusivities evaluated at high moisture levels from a series of water absorption tests. *Mater Struct* 35(3):141–148
- Kodikara J, Chakrabarti S (2005) Modeling of moisture loss in cementitious stabilized pavement materials. *Int J Geomech* 5(4):295–303
- Sant G, Eberhardt A, Bentz A, Weiss J (2010) Influence of shrinkage-reducing admixtures on moisture absorption in cementitious materials at early ages. *J Mater Civ Eng ASCE* 22(3):277–286
- Ayano T, Wittmann FH (2002) Drying, moisture distribution, and shrinkage of cement-based materials. *Mater Struct* 35(3):134–140
- Luo R, Niu JL (2004) Determination of water vapor diffusion and partition coefficients in cement using one FLEC. *Int J Heat Mass Transf* 47(10–11):2061–2072
- Aquino W, Hawkins NM, David AL (2004) moisture distribution in partially enclosed concrete. *ACI Mater J* 101(4):259–265
- Garbalinska H (2002) Measurement of the mass diffusivity in cement mortar: use of initial rates of water absorption. *Int J Heat Mass Transf* 45(6):1353–1357
- Nilsson LO (2002) Long-term moisture transport in high performance concrete. *Mater Struct* 35(10):641–649
- Anderberg A, Wadsö L (2008) Method for simultaneous determination of sorption isotherms and diffusivity of cement-based materials. *Cem Concr Res* 38(1):89–94
- Zaknune A, Glouannec P, Salagnac P (2012) Estimation of moisture transport coefficients in porous materials using experimental drying kinetics. *Int J Heat Mass Transf* 48(2):205–215
- Tada S, Watanabe K (2005) Dynamic determination of sorption isotherm of cement based materials. *Cem Concr Res* 35(12):2271–2277
- Arambula E, Caro S, Masad E (2010) Experimental measurement and numerical simulation of water vapor diffusion through asphalt pavement materials. *J Mater Civ Eng ASCE* 22(6):588–598
- Evangelides C, Arampatzis G, Tzimopoulos C (2010) Estimation of soil moisture profile and diffusivity using simple laboratory procedures. *Soil Sci* 175(3):118–127
- Fanek H, Fava C, Huang EC (2012) Determination of effective diffusion coefficient of water in marshmallow from drying data using finite difference method. *Int Food Res J* 19(4):1351–1354
- BS EN 15206 (2007) Hygrothermal performance of building components and building elements: Assessment of moisture transfer by numerical simulation. BSI, London
- Derluyn H, Derome D, Carmeliet J, Stora E, Barbarulo E (2012) Hysteretic moisture behavior of concrete: modeling and analysis. *Cem Concr Res* 42(10):1379–1388
- Nguyen TQ, Petkovic J, Dangla P, Baroghel-Bouny V (2008) Modelling of coupled ion and moisture transport in porous building materials. *Constr Build Mater* 22(11):2185–2195
- Baroghel-Bouny V, Thiéry M, Wang X (2011) Modelling of isothermal coupled moisture-ion transport in cementitious materials. *Cem Concr Res* 41(8):828–841

39. Bazant ZP, Najjar LJ (1972) Nonlinear water diffusion in non-saturated concrete. *Mater Struct* 5(25):3–20
40. Martin-Perez B, Pantazopoulou SJ, Thomas MDA (2001) Numerical solution of mass transport equations in concrete structures. *Comput Struct* 79(13):1251–1264
41. Bazant ZP, Najjar LJ (1971) Drying of concrete as a nonlinear diffusion problem. *Cem Concr Res* 1(5):461–473
42. Janssen H, Blocken B, Carmeliet J (2007) Conservative modelling of the moisture and heat transfer in building components under atmospheric excitation. *Int J Heat Mass Transf* 50(5–6):1128–1140
43. Conciatori D, Sadouki H, Brühwiler E (2008) Capillary suction and diffusion model for chloride ingress into concrete. *Cem Concr Res* 38(12):1401–1408
44. Claisse PA, Eisayad BI, Shaaban IG (1997) Absorption and sorptivity of cover concrete. *J Mater Civ Eng ASCE* 9(3):105–110
45. Iqbal PO, Ishida T (2009) Modeling of chloride transport coupled with enhanced moisture conductivity in concrete exposed to marine environment. *Cem Concr Res* 39(4):329–339
46. Martys N, Ferraris CF (1997) Capillary transport in mortar and concrete. *Cem Concr Res* 27(5):747–760
47. Wang BX, Fang ZH (1988) Water absorption and measurement of the mass diffusivity in porous media. *Int J Heat Mass Transf* 31(2):251–257
48. Akita H, Fujiwara T, Ozaka Y (1997) A practical procedure for the analysis of moisture transfer within concrete due to drying. *Mag Concr Res* 49(179):129–137
49. Buchwald A (2000) Determination of the ion diffusion coefficient in moisture and salt loaded masonry materials by impedance spectroscopy. In: *Proceedings of third international symposium, Vienna*, p 475–482
50. Hall C, Hoff WD (2002) *Water transport in brick, stone, and concrete*. Spon Press, London
51. Prazak J, Tywoniak J, Peterka F, Slonc T (1990) Description of transport of liquid in porous media—a study based on neutron radiography data. *Int J Heat Mass Transf* 33(6):1105–1120
52. Martin-Perez B (1999) *Service life modelling of R.C. highway structures exposed to chlorides*, Ph.D. thesis, University of Toronto, Toronto
53. Kodikara J, Chakrabarti S (2005) Modeling of moisture diffusion in crushed basaltic rock stabilized with cementitious binders. *J Mater Civ Eng ASCE* 17(6):703–710
54. Morgan RD (1988) *Dry-mixed silica fume shotcrete in Western Canada*. *Concr Int* 10(1):24–32
55. Roy SK, Northwood DO, Aldred JM (1995) Relative effectiveness of different admixtures to prevent water penetration in concrete. In: *Proceedings of a conchem conference Brussels, Belgium*, pp 451–459